Oil & Gas Science and Technology - Rev. IFP Energies nouvelles **74**, 67 (2019)

https://doi.org/10.2516/ogst/2019034

Available online at:
ogst.ifpenergiesnouvelles.fr

REGULAR ARTICLE

OPEN ACCESS

Probabilistic approach of a flow pattern map for horizontal, vertical, and inclined pipes

Rafael Amaya-Gómez[1,2,*], Jorge López[3], Hugo Pineda[1], Diana Urbano-Caguasango[1], Jorge Pinilla[1], Nicolás Ratkovich[1], and Felipe Muñoz[1]

[1] Department of Chemical Engineering, Universidad de los Andes, Cra 1E # 19A -40, Bogotá, Colombia
[2] Université de Nantes, GeM, Institute for Research in Civil and Mechanical Engineering, CNRS UMR 6183, BP 92208 – 44322 Nantes Cedex 3, France
[3] McDougall School of Petroleum Engineering, The University of Tulsa, 800 South Tucker Drive, NCDB 105D, Tulsa, 74104 OK, USA

Received: 26 October 2018 / Accepted: 14 May 2019

Abstract. A way to predict two-phase liquid-gas flow patterns is presented for horizontal, vertical and inclined pipes. A set of experimental data (7702 points, distributed among 22 authors) and a set of synthetic data generated using OLGA Multiphase Toolkit v.7.3.3 (59 674 points) were gathered. A filtering process based on the experimental void fraction was proposed. Moreover, a classification of the pattern flows based on a supervised classification and a probabilistic flow pattern map is proposed based on a Bayesian approach using four pattern flows: Segregated Flow, Annular Flow, Intermittent Flow, and Bubble Flow. A new visualization technique for flow pattern maps is proposed to understand the transition zones among flow patterns and provide further information than the flow pattern map boundaries reported in the literature. Following the methodology proposed in this approach, probabilistic flow pattern maps are obtained for oil–water pipes. These maps were determined using an experimental dataset of 11 071 records distributed among 53 authors and a numerical filter with the water cut reported by OLGA Multiphase Toolkit v7.3.3.

1 Introduction

Liquid-gas multiphase flows are complex physical processes that depend on how the interface deforms, the flow direction, and the compressibility of one of the phases (in some cases). Given certain operating conditions such as pressure, temperature, liquid or gas velocity, pipe orientation, and fluid properties, several interfacial geometric configurations have been reported in two-phase flow systems. These configurations are commonly known as flow patterns or flow regimes. Some of the reported patterns for vertical flow are bubble flow, slug flow, churn flow, wispy-annular flow, and annular. Whereas for horizontal flow, the patterns include bubble flow, plug flow, stratified flow, wavy flow, slug flow, and annular [1, 2]. Prediction of these patterns is a matter of concern for designers and operators considering their relation to pressure drop and heat transfer calculations [3–7].

Two-dimensional flow pattern maps serve to visualize the most likely liquid-gas flow pattern found in a section of constant diameter, inclination, fluid properties, and input volumetric gas and liquid flow rates. These maps are usually developed based on measurable parameters along the pipeline segment instead of dimensionless variables such as the Weber, Froude, or Lockhart Martinelli numbers [8, 9]. For instance, Taitel and Dukler [10] proposed a map using superficial velocities; Baker [2] and Hewitt and Roberts [11] developed maps using mass velocities; and Kattan *et al.* [4–6] and Cheng *et al.* [3, 12] considered flow pattern maps based on mass fluxes. Depending on the information used to develop these maps, they can be classified into experimentally or mechanistic-based. The first is obtained from a significant number of experiments, whereas the second is built up from the examination of transition mechanisms using fundamental equations [1]. The commonly implemented flow pattern maps for vertical pipes are those reported by Govier *et al.* [13], Griffith and Wallis [14], Hewitt and Roberts [11], Golan and Stenning [15], Oshinowo and Charles [16], Taitel *et al.* [17], Spedding and Nguyen [18], Barnea *et al.* [19], Spisak [20], Ulbrich [21], and Dziubinski *et al.* [22]. For horizontal and near horizontal pipes, the maps of Baker [23], Taitel and Duker [10], Hashizume [24], and Steiner [25] are often quoted [26]. Finally, for inclined pipes, the maps of Shoham [9], Magrini [27] and Mukherjee [28] are commonly preferred.

Despite the diversity of experimental flow pattern maps, different authors have criticized the subjectivity of these maps due to identification techniques like visual inspection [29]. Therefore, numerical methods, which discretize and

* Corresponding author: r.amaya29@uniandes.edu.co

solve commonly accepted equations of flow dynamics, have also been considered to set up approaches like the two-phase model [29]. Simulation tools like OLGA, LedaFlow, PeTra, and fluid dynamic simulators such as CFD codes using Eulerian formulations have been reported in the literature to simulate the behavior of these multiphase flows [30–36]. Nevertheless, these simulators are commonly designed for pipelines with large diameters and risers, so over-predictions of the void fraction may occur [37].

Although different flow pattern maps are available, there are still difficulties in defining common boundaries between flow regimes [29]. Usually, these boundaries differ significantly among maps reported, and wide transition areas can be obtained; even flow patterns have been suggested to follow a combination and not standalone regimes [38]. Therefore, efforts should focus on determining which is the predominant flow regime, and a probabilistic-based map can be considered in advance. In this direction, a few pieces of work using R134a, R410A, and air–water have been proposed [39–43]. These works evaluate the probability of a flow regime under some operating conditions and flow quality based on a sequence of experimental images. However, probabilistic flow pattern maps based on extensive experimental and synthetic databanks aiming to assess transition zones have not been developed yet. Accordingly, the present work aims to develop a probabilistic-based approach to identify the more likely flow regime under some operating conditions. To this end, experimental records from an extensive literature review and synthetic data from OLGA v.7.3.3 simulations were implemented. *Oil and Gas Simulator-Schlumberger (OLGA)* was selected because is one of the commonly implemented simulators in the *Oil and Gas industry* and its good agreement with experimental results [32, 33].

This paper is organized as follows: Section 2 contains a review of flow pattern maps and their classification. Section 3 describes the experimental and synthetic datasets. Section 4 presents the flow pattern probabilistic-based approach. Section 5 summarizes the basic findings and presents suggestions for future work. Besides, the paper counts with three appendices associated with the procedure developed to estimate the posterior probability (Appendix A.1 in Supplementary Material), the probabilistic flow pattern maps with several inclinations (Appendix A.2 in Supplementary Material), and the pattern maps for liquid-liquid flow following a parallel approach (Appendix A.3 in Supplementary Material).

2 Review of flow pattern map classification

2.1 Horizontal flow patterns

According to authors like França and Lahey [44], Zhang *et al.* [45], and Fan [46], horizontal flow patterns can be classified as follows: stratified smooth flow, stratified wavy flow, elongated bubble flow or plug flow, slug flow, annular flow, and wavy annular flow. These flow patterns can be grouped based on the following considerations: (i) Intermittent flow patterns cover plug and slug flow, as in vertical cases, because they are composed of large bubbles (Taylor bubbles), which are followed by a series of smaller bubbles. The main difference between the plug and slug flow patterns lies in the shape of the elongated bubble and the turbulence generated behind it; (ii) like in vertical pipes, the bubbly flow pattern refers to small spherical bubbles; and (iii) segregated flow patterns, both smooth and wavy, exhibit a clear separation of the liquid and gas phases, which creates a distinct interface between them. For the wavy case, increasing the gas velocity destabilizes the interface and creates waves in the liquid surface [47, 48]. This distinction, however, is not significant for the current work [49]. The flow patterns found in the literature can be grouped then as follows (Tab. 1): Segregated Flow, Intermittent Flow, and Bubbly Flow [49].

This classification discriminates the available flow regimes clearly, so it will be used to gather experimental information. Besides, these flow regimes are reported by OLGA; hence, a direct comparison between synthetic and experimental data becomes possible. A graphical scheme of these flow patterns is depicted in Figures 1a–1c.

2.2 Vertical flow patterns

Vertical two-phase flows are commonly classified as bubbly flow, slug flow, churn flow, wispy annular flow, and annular flow. This classification has been proposed by different author and it can be seen in Taitel and Dukler [10], Carey [50], Ghajar [8] and Falcone *et al.* [51]. Authors such as Kouba [52], Thomas [53], Omebere-Iyari and Azzopardi [54], and Rosa *et al.* [55] have proposed minor changes of the flow patterns aforementioned. Therefore, a grouping criteria similar to the reported by Inoue *et al.* [49] is considered.

The flow patterns are grouped based on the following considerations: (i) The dispersed bubbles (bubbly flow) covers isolated bubbles sparsely distributed over the pipe cross-section, as a cluster of bubbles known as discrete bubbles. Isolated bubbles refer to uniformly sized bubbles describing a straight path, which does not interact with each other. (ii) A cluster of bubbles refers to non-spherical bubbles with non-uniform size distribution. Factors such as slipping between phases, which were identified by Omebere-Iyari and Azzopardi [54], seem to make sense only for situations where the liquid flows at low velocities. This situation is not of practical importance; therefore, it is not considered in the current grouping criteria. (iii) Intermittent flow pattern encompasses slug flow, churn flow, and unstable churn flow. This grouping criterion is undertaken considering that authors who identify these patterns described consistently liquid pistons of considerable length (large and elongated bubbles) followed by smaller bubbles, which are usually spherical. The pattern "slug flow" corresponds to Taylor bubbles; these bubbles occupy much of the cross-section, followed by smaller spherical bubbles. The pattern churn flow corresponds to the destabilization of Taylor bubbles, followed by small, destabilized bubbles. Finally, the unstable churn flow pattern, identified by Rosa *et al.* [55], describes coalescence of the Taylor bubbles with the small bubbles. (iv) Kouba [52] and Rosa *et al.* [55] used semi-annular flow to describe the pattern that occurs between the unstable "churn" and the smooth annular pattern. Semi-annular flow is regarded as a degenerate form

Table 1. Flow pattern classification for horizontal pipes used in this work. Adapted from Inoue *et al.* (2013) [49].

Pattern	Representation in the literature			
	França and Lahey (1992)	Zhang *et al.* (2003)	Thomas (2004)	Fan (2005)
Segregated Flow (SG)*	Stratified-smooth flow Stratified-wavy flow	Stratified flow –	Stratified smooth –	Stratified-smooth flow Stratified-wavy flow
Intermittent Flow (IT)	Plug flow Slug flow	Slug flow –	Slug flow –	Slug flow –
Bubbly Flow (BF)	–	Dispersed bubble flow	Dispersed bubble flow	Bubble flow

*Annular flow can be classified as segregated flow.

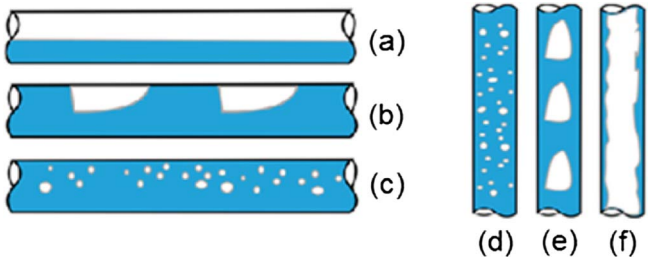

Fig. 1. Graphical representation of the horizontal and vertical flow patterns (a) Segregated Flow. (b) Horizontal Intermittent Flow. (c) Horizontal Bubbly Flow. (d) Vertical Bubbly Flow. (e) Vertical Intermittent Flow. (f) Annular Flow.

of annular flow with high waves in the liquid–gas interface [12, 28]. For this application, this pattern is grouped as an annular flow.

Based on these considerations, the different flow patterns found in the literature can be grouped as (Tab. 2): Bubbly Flow, Intermittent Flow, and Annular Flow [49], graphically shown in Figures 1d–1f.

For inclined pipes, both the flow patterns presented in the horizontal and vertical orientations will be used.

3 Experimental and synthetic datasets

3.1 Experimental dataset

The experimental dataset has 7702 records distributed among 22 authors as shown in Table 3. These authors performed measurements for different liquid-gas combinations (covering refrigerants to viscous oils), superficial velocities, pipe lengths, and diameters. However, the water–air system is the most frequently used combination with about 62% of all the gathered records. Table 3 also presents pipes orientation during the experiments, which include vertical, horizontal, and inclined pipes with upward and downward directions. As expected, a larger number of data points is reported for horizontal cases and a lower amount of records for vertical downward pipes (−90°).

Figure 2 depicts other relevant parameters of the experimental dataset: the distribution for the diameter, L/D relation, and superficial velocities. Note that the pipe diameters follow commercial dimensions (*i.e.*, 1 in., 2 in. and 2.5 in.), and the mean L/D relation is 455, which ensures flow development for most of the cases. Besides, the flow patterns were classified as Annular flow in 23%, Segregated flow in 21%, Bubbly flow in 14% and Intermittent flow in 42%.

Table 2. Flow pattern classification for vertical pipes used in this work. Adapted from Inoue *et al.* (2013) [49].

Pattern	Representation in the literature					
	Kouba (1986)	Carey (1993)	Thomas (2004)	Omebere-Iyari and Azzopardi (2007)	Falcone *et al.* (2009)	Rosa *et al.* (2010)
Bubbly Flow (BF)	– Dispersed bubble flow	– Bubbly flow	– Bubbles	Dispersed bubbles Bubble flow	– Bubble flow	Spherical caps Bubbly flow
Intermittent Flow (IT)	Elongated bubble flow Slug flow	Slug flow Churn flow	Slug flow Churn flow	Slug flow Churn flow	Slug flow Churn flow	Stable slug Unstable slug
Annular Flow (AF)	Wavy annular flow Annular flow	Wispy annular flow Annular flow	Annular flow –	Annular flow –	Wispy annular flow Annular flow	Semi annular Annular

Table 3. Experimental data.

Author	Data	Fluids	Diameter [mm]	L/D	VsL [m/s]	VsG [m/s]	θ [°]	Void fraction
Abduvayt *et al.* [56]	443	Water–nitrogen	54.9–106.4	939.85–1821.49	0.009–6.48	0.04–11.10	0–3	NR*
Badie *et al.* [57]	66	Oil, water–air	78	474.36	0.001–0.05	14.76–25.27	0	0.89–0.995
Beggs [58]	323	Water–air	25.4–38.1	720.00–1080	0.0005–58.25	0.02–32.11	0–90	0.094–1.00
Carvalho *et al.* [59]	59	Water–air	60	23.67	0.506–4.20	0.02–2.84	−90	0.005–0.976
Fan [46]	351	Water–air	50.8–149.6	748.03–754.01	0.0003–0.05	4.93–25.70	−2 to 2	0.856–0.998
Felizola [60]	89	Kerosene–air	51	294.12	0.050–1.49	0.39–3.36	0–90	0.323–0.798
França and Lahey [44]	99	Water–air	19	96.32	0.010–14.85	0.13–23.76	0	0.063–0.944
Ghajar [7]	166	Water–air	12.7	123.94	0.080–1.17	0.19–20.06	0/90	0.036–0.916
Gokcal [61]	356	Oil–air	50.8	372.05	0.010–1.76	0.09–20.30	0	0.01–0.89
Kouba [52]	53	Kerosene–air	76.2	5480.00	0.152–2.14	0.30–7.36	0	NR
Magrini [27]	140	Water–air	76.2	229.66	0.003–0.04	36.63–82.32	0–90	0.976–0.998
Majumder *et al.* [62]	99	Amylic alcohol, glycerin–air	19.05	178.48	0.585–2.34	0.08–0.70	90	0.13–0.52
Manabe *et al.* [63]	247	Oil–natural gas	54.9	357.01	0.038–0.95	0.10–7.01	0–90	NR
Meng [47]	203	Oil–air	50.1	377.25	0.001–0.05	4.80–26.60	0	0.786–0.999
Mukherjee [28]	872	Kerosene, lube oil–air	38.1–101.6	129.17–1360	0.009–4.36	0.01–36.26	−70 to 90	0.01–1.00
Omebere-Iyari and Azzopardi [54]	98	Naphtha – nitrogen	189	275.13	0.004–4.34	0.09–15.63	90	NR
Rosa *et al.* [55]	73	Water–air	26	257.69	0.220–3.08	0.12–28.80	90	0.02–0.87
Roumazeilles [64]	113	Kerosene–air	51	372.55	0.884–2.44	0.91–9.36	−30 to 0	0.264–0.867
Schmidt *et al.* [65]	87	Povidone and water–nitrogen	54.5	56.88	0–3.42	0.05–29.58	90	0.02–0.96
Shoham [9]	3551	Water–air	25–51	196.08–400	0.002–25.52	0.004–42.96	−90 to −90	NR
Tanahashi *et al.* [66]	11	Water–air	54	92.59	0.258–0.27	0.04–0.16	90	NR
Wilkens [67]	203	Saltwater–CO_2	97.2	185.00	0.095–1.57	0.80–13.61	−2 to 5	NR

* NR, non-reported.

3.2 Selection of flow pattern map axis

Non-slip void fraction is one of the top parameters used to characterize two-phase flows, *i.e.*, to obtain two-phase relative velocity, and to predict flow pattern transitions [48, 68]. Void fraction depends on different physical parameters (*e.g.*, gas/liquid velocities and viscosities) and operational parameters (*e.g.*, pipeline length and diameter) [69].

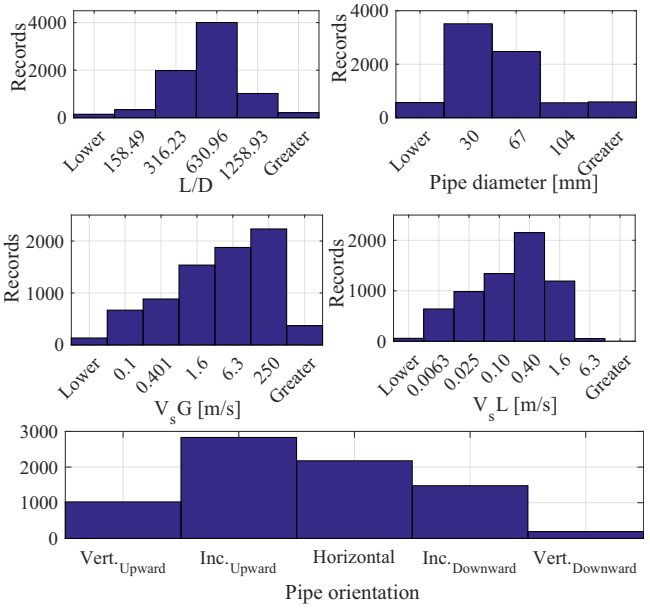

Fig. 2. Distribution of the experimental data listed in Table 3.

In this work, the void fraction is used to compare the experimental and synthetic records; however, this parameter is often ignored in experimental works [29]. Therefore, this approach focused on a flow pattern map in which the axis features better describe the void fraction.

For this purpose, gas/liquid superficial velocities were used to build the flow pattern map given to their relevance in the void fraction prediction. This pattern flow map is one of the most common coordinates in the literature, given its physical representation and experimental reproduction [54–57, 62, 63]. This selection is supported by a feature selection based on a predictor importance analysis, which characterizes the general effect of the experimental void fraction.

3.3 Synthetic dataset

The steady-state synthetic records were generated with OLGA Multiphase Toolkit v.7.3.3 obtaining 59 574 records with the main parameters depicted in Table 4. The effect of pipe inclination on the flow pattern was evaluated by considering 5° steps from −90° to 90°. The remaining required parameters, except for the gas and liquid superficial velocities, were randomly selected based on the ranges obtained in the experimental database. This procedure aims to perform a correct overlap between the experimental and synthetic data by setting the gas velocity from 1e-02 to 40 m/s and the liquid velocity from 1e-03 to 68 m/s. These ranges were chosen based on the available experimental data. Transitions between neighboring flow patterns were represented by a mesh rather than a boundary line. This mesh was refined with synthetic data in those locations where transition zones appeared on the available experimental dataset for every inclination, *i.e.*, a higher number of records of two flow patterns.

3.4 Experimental data processing

A filtering process was used to select the experimental records within an acceptable error in the void fraction prediction. This acceptable error is determined based on a tolerable difference between experimental and synthetic predictions of the void fraction. However, 4407 experimental records did not report this parameter, and a direct classification is not possible; therefore, a supervised learning approach was used to classify those records as acceptable/non-acceptable for the construction of the flow pattern map. For this purpose, experimental records already classified as acceptable or non-acceptable were used as a training set.

For the classification process, two types of supervised classifiers were considered: (i) Support Vector Machines (SVM) and (ii) K-Nearest Neighbors (KNN). These techniques have also been used in multiphase flow data classification [70, 71]. A SVM classifier maps a given set of binary labeled training data into a high dimensional feature space, and it separates the classes with a maximum margin hyperplane [72]. KNN is a classification based on a majority vote of its K neighbors [73]. Further details about the mathematical description of these classifiers are found in Duda *et al.* [74], Tarca *et al.* [70], and Zhang and Wang [71]. The main features of these processes are described below.

The SVM classifier was developed following the recommendations reported by Hsu *et al.* [75]. A Radial Basis Function (RBF) was implemented because, (i) this kernel can handle a nonlinear classification, (ii) it has fewer hyperparameters comparing with other kernel functions (*e.g.*, polynomial), and (iii) it has fewer numerical difficulties. Moreover, sensibility analyses were implemented to determine the penalty (C) and the RBF parameters (γ) to minimize the classification error. For this purpose, a Cross-Validation process with an exponentially growing sequence (*i.e.*, $C \in (2^{-1}, 2^{0},\ldots, 2^{4})$ and $\gamma \in (2^{-2}, 2^{-1},\ldots, 2^{3})$) were considered obtaining that $C = 16$ and $\gamma = 0.25$ achieve the greater prediction rate. For the KNN classifier, the number of neighbors for the voting process was evaluated to obtain an accurate classification rate; therefore, a sensibility analysis was performed obtaining that a nine-neighbors classification has the lowest misclassified rate. The two classifiers (*i.e.*, SVM, and KNN) were implemented following a 10-fold Cross-Validation process to compare their rates of classification.

Three criteria were considered to determine the tolerable error: (i) acceptable records are included as much as possible; (ii) tolerable error should be as low as possible; and (iii) the performance of the classifier should be as good as possible. Based on these criteria, a performance classifier was proposed:

$$C_Q = (1 - \epsilon_{\text{tol}}) \times \text{CP} \times \text{AD}, \tag{1}$$

where C_Q represents the classifier quality [%], ϵ_{tol} is the evaluated tolerable error [%], CP is the classifier performance [%] (related to the accurate rate), and AD is the acceptable data [%]. This criterion was evaluated in an error span from 0% to 50% because more than 90% of experimental records were included therein (see Fig. 3).

Table 4. Comparison among Experimental and Synthetic Datasets parameters.

Dataset parameter	Experimental			Synthetic		
	Minimum	Maximum	Average	Minimum	Maximum	Average
Diameter [m]	0.0127	0.189	0.046	0.0127	0.18	0.053
Length [m]	1.42	418	23.79	1.5	417	39.19
Liquid superficial velocity [m/s]	0	68.2	0.86	0.001	59.43	8.86
Gas superficial velocity [m/s]	0.00372	82.3	7.18	0.01	39.81	5.94
Liquid density [kg/m^3]	49.4	1090	943.57	702.3	1053.9	955.88
Gas density [kg/m^3]	0.91	103	4.54	1.1	24.45	15.92
Liquid composition	0	1	0.19	0	1	–
Liquid viscosity [Pa s]	0.000325	6.88	0.03	0.00036	0.05654	0.007
Gas viscosity [Pa s]	0.00001	0.00117	0.000029	0.000013	0.000019	0.000016
Superficial tension [N/m]	0.001	0.929	0.063	0.0028	0.078	0.043
Inclination [°]	−90	90	11.53	−90	90	−2.58
Void fraction	0.00516	1	–	0	1	–
Pressure [bar]	0.0667	90	4.04	0.0667	90	13.03
Temperature [K]*	255	373	300.84	–	–	–

* Temperature was not used for OLGA calculations.

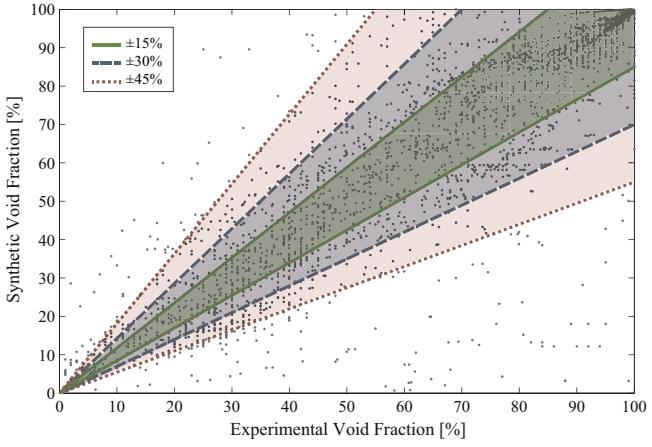

Fig. 3. Experimental and synthetic void fraction comparison.

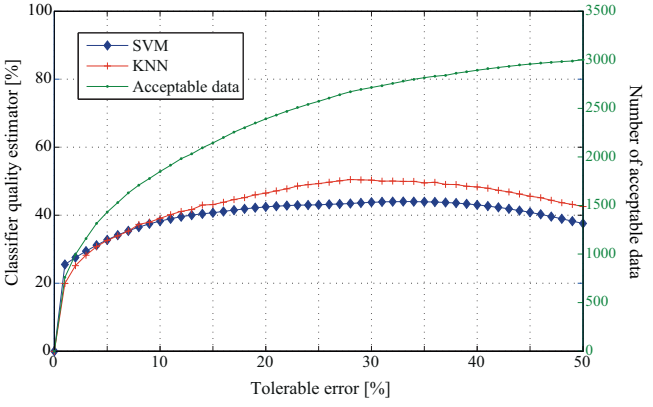

Fig. 4. Tolerable error determination by the classifier quality estimator.

Equation (1) uses the residual of the tolerable error because this is the only parameter that is wanted to be the lowest as possible, in contrast to the classifier performance and the acceptable data, where these parameters are sought to be the highest. Based on the results from this quality estimator (Fig. 4), the KNN classifier has the best performance with a tolerable error between 25% and 30%. Following expert criteria, the tolerable error was set at 25%, *i.e.*, every experimental measurement with an error percent below 25% was classified as acceptable, otherwise as not acceptable. The non-acceptable records include around 75% of the data reported by Majumder (Kerosene, Lube Oil/Air) and Schmidt (Povidone Water/Nitrogen), 146 records for upward directions between 5° and 90°, 209 of nearly horizontal records (−5° to 5°), and 138 records of downward experiments (−90° to −5°). These records correspond to 309 records with a diameter lower than 30 mm, 394 records within 30–60 mm, and only one record greater to 100 mm. Regarding the fluid velocities and the void fraction, the *VsL* and *VsG* had a greater proportion between 1e-01 and 1 m/s, and the majority of the records (63%) had a void fraction lower to 0.5. After the supervised classification, a total of 5806 over 7702 acceptable records were obtained, which corresponds now on as the experimental dataset for the flow pattern map construction.

4 Flow pattern map probabilistic-based approach

4.1 Experimental-synthetic dataset overlapping

OLGA's Multiphase Toolkit point model was used to calculate the fully developed steady-state operating conditions in a straight pipe. It operates with nine gas/liquid flow regimes [76]: 0. Stratified smooth; 1. Stratified wavy; 2. Annular; 3.

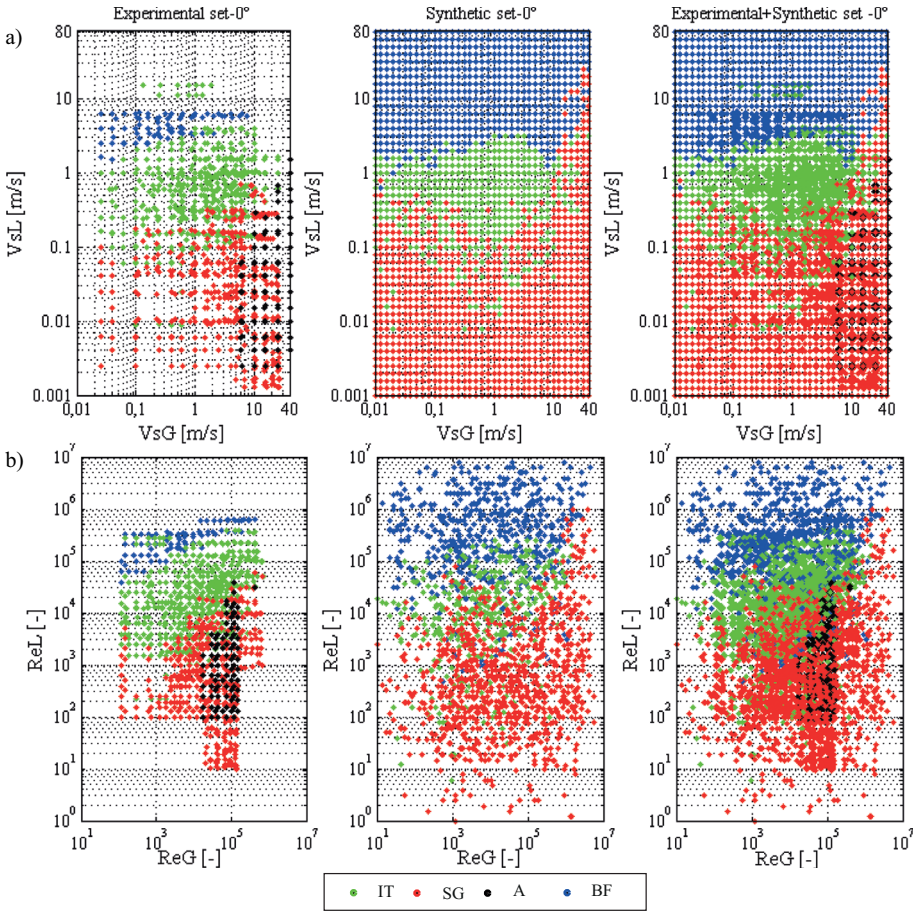

Fig. 5. Experimental and synthetic a) superficial velocities and b) Reynolds flow pattern map for horizontal pipes.

Slug flow; 4. Bubble flow; 5. Two-phase oil/water; 6. Single phase gas; 7. Single phase oil; and 8. Single phase water. For this work, it was not contemplated the flow regimes 5, 6, 7, and 8, whereas the flow regimes 0 and 1 were coupled as one flow regime (Stratified). For the sake of simplicity, the flow regimes are denoted in this work as 0 (Segregated Flow) – SG; 2 (Annular Flow) – A; 3 (Intermittent Flow) – IT; and 4 (Bubble Flow) – BF. The OLGA Multiphase Kit assumes that for vertical or near vertical (±75° or more) there is not segregated flow, but only annular flow. This assumption is linked to the gravitational forces that impede to observe this phase for these inclinations (as in Fig. 1d). In these cases, the annular flow represents specific types of segregated phases. For horizontal cases, OLGA does not recognize an annular flow pattern, and this pattern is grouped with the segregated flow pattern (0 or SG) [76, 77].

The experimental and synthetic datasets overlapping for a horizontal pipe are shown in Figure 5a based on superficial velocities and Figure 5b Reynold numbers. These figures show that the experimental and the synthetic datasets mainly agree in their flow regimes, and only an experimental subset was misclassified by predicting an annular flow, which is a flow pattern that was not obtained in the synthetic dataset. Nevertheless, it should be pointed out that it is not possible to generate a grid for the synthetic dataset using the Reynolds number since the randomization of the fluid combinations would generate nonphysical superficial velocities to match a certain Reynolds number. This impossibility is generated mainly by the liquid viscosity, which varies in several orders of magnitude.

4.2 Probabilistic flow map

The primary location of the flow regimes can be determined through the distribution depicted in Figure 5; however, this map cannot assess transition areas yet, and points may be overlapped. Then, an alternative visualization is proposed base on the Probability Density Functions (PDF) of each flow pattern for both liquid and gas velocities. These pdfs are determined from empirical distributions using histograms and cubic splines to obtain smoother results. The obtained results are shown in Figure 6, where it can be seen that an overlapping classification over the transition areas between two flow patterns exists. For example, it can be seen that Segregated (SG) and Annular (A) flow regimes transition area is mostly located in a gas velocity above of 10 m/s and a liquid velocity of 0.01 m/s. Although this map provides useful information about the overall transition areas for all possible values of the liquid or gas veloci-

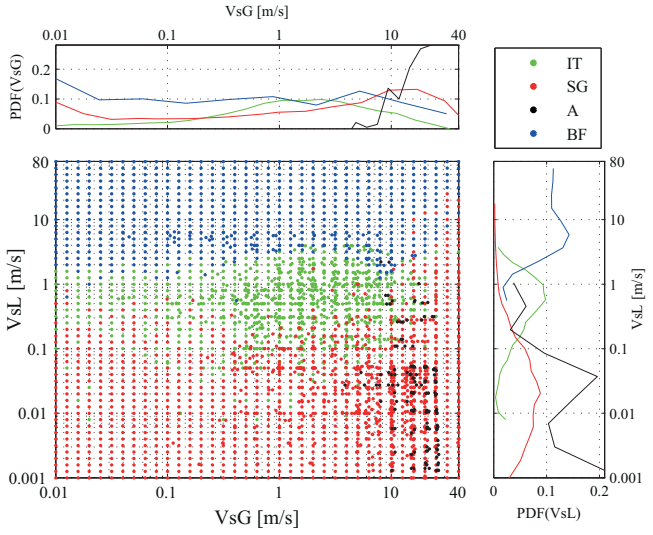

Fig. 6. Flow pattern map for horizontal pipes with pdfs' for gas and liquid velocities.

ties, the specific transition area between two flow patterns could not be assessed, and there is still a great uncertainty surrounding the classification results. Therefore, an alternative map was proposed to identify these transition areas regardless of an overlapping problem. A translucent flow pattern map with contour lines was suggested for this purpose.

To obtain the translucent flow pattern map, a refined mesh of 200 901 elements (matrix of 501 rows and 401 columns) was developed. This mesh determines the number of points over the entire span of velocities for every flow regime. Projected surfaces for each flow pattern were developed – using a specific level of transparency given their

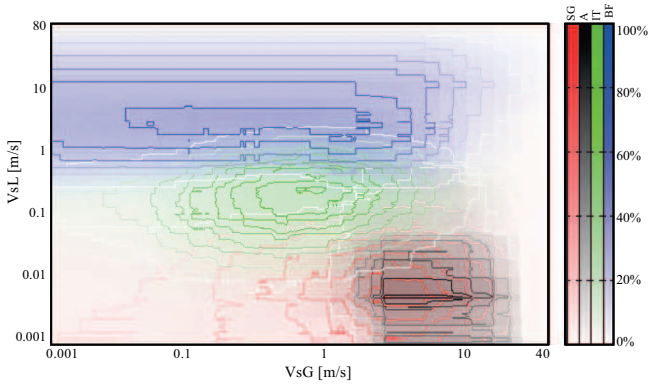

Fig. 7. Translucent flow pattern map.

order of appearances –, and contour lines were added to these surfaces to show the concentration levels of each regime. The translucent obtained map is shown in Figure 7. Note that an important number of measurements are located in two transition areas between different contour regimes.

A probabilistic approach based on the aforementioned refined mesh and a Bayesian approach is proposed to deal with the transition areas. According to the Bayes formula, a posterior probability could be determined as [74]:

$$P(Y=y|X=x)=\frac{P(X=x\mid Y=y)P(Y=y)}{\sum_{\forall i\in Y}P(X=x\mid Y-i)P(Y=i)}, \tag{2}$$

where $P(Y=y)$ is the prior probability of belonging to category y, $P(X=x|Y=y)$ is known as the likelihood function, $P(Y=y|X=x)$ is the posterior probability, and $\sum_{\forall i\in Y}P(X=x|Y-i)P(Y=i)$ is known as the

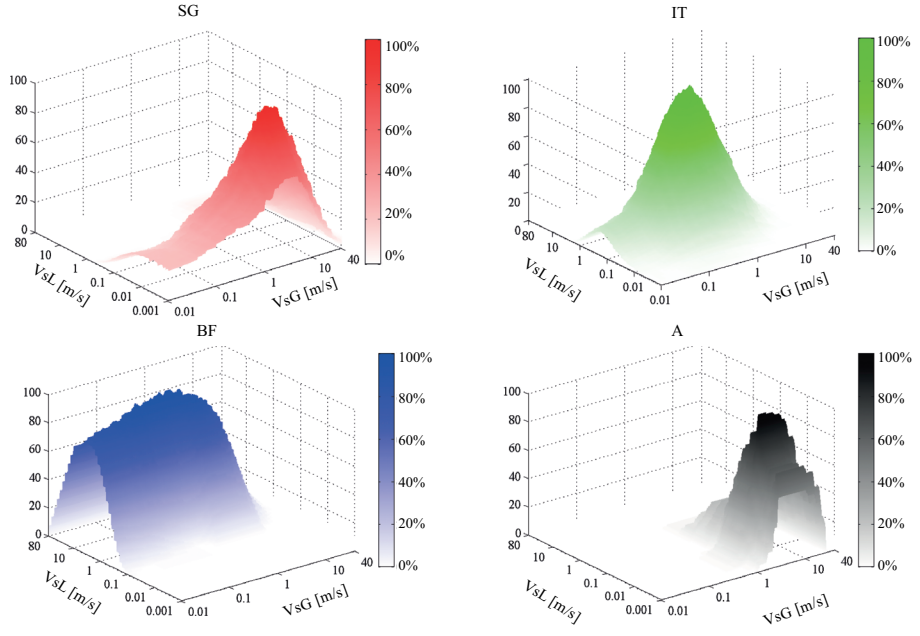

Fig. 8. Flow patterns surfaces.

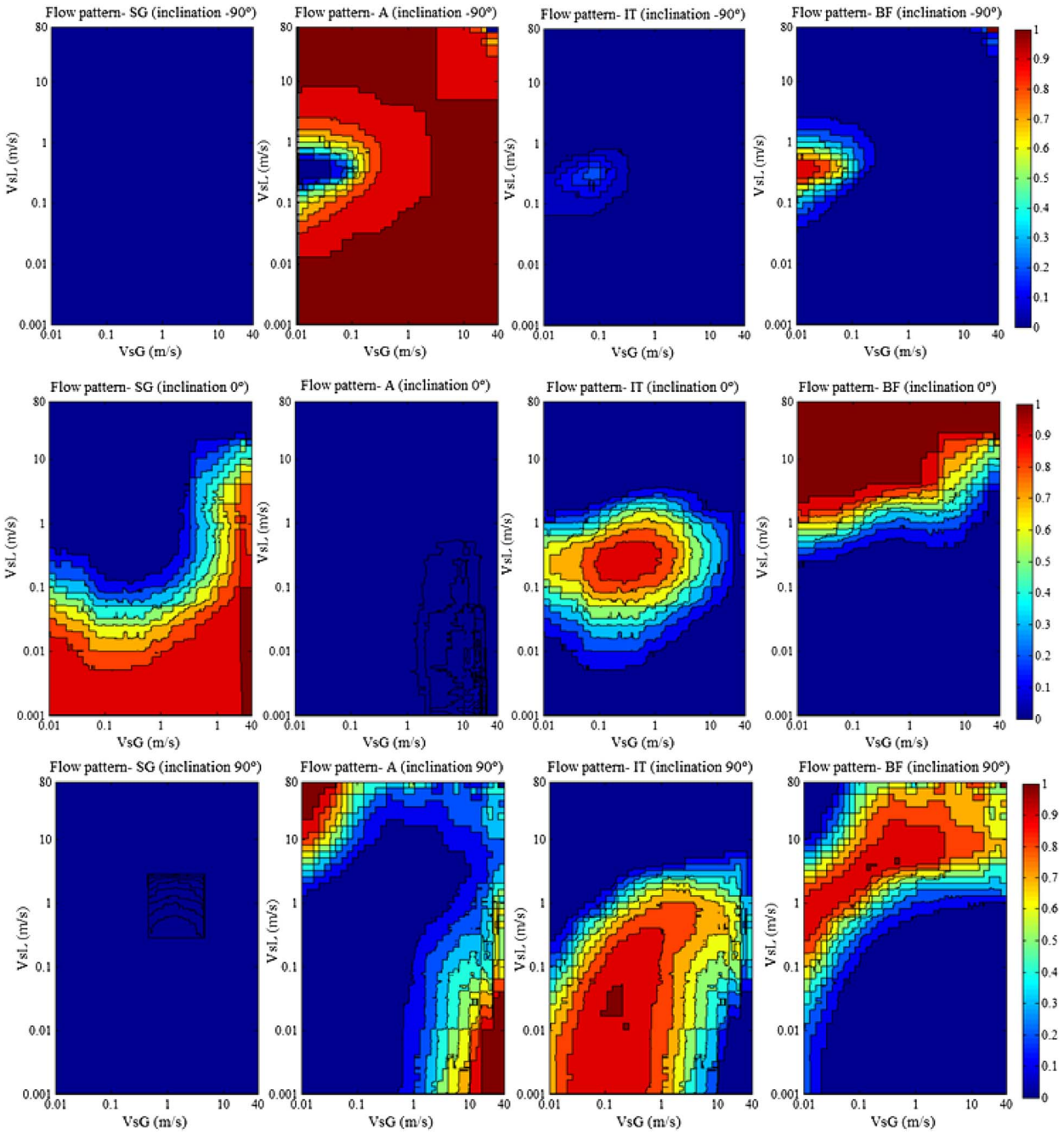

Fig. 9. Probability flow pattern map results for −90°, 0° and 90°.

evidence, however, it can be viewed as a scale factor for the posterior probability.

The following considerations were implemented to calculate the posterior probability for every flow pattern:

1. The prior probabilities were obtained by the ratio between the number of points in the category y (N_y) and the total number of points (N_T).
2. The likelihood function is a term chosen to indicate that the category for which it is large is more "likely" to be the correct category [74]. Therefore, surfaces from a refined mesh were obtained for all regimes, as is depicted in Figure 8. $Z_y(i, j)$, denotes the height of the surface from the flow regime for a given liquid and gas velocities (i, j).

Appendix A.1 in Supplementary Material describes with more details the proposed procedure.

The probabilistic flow pattern map was determined for every flow regime for an inclination of −90° (vertical downward pipe), 0° (horizontal pipe) and 90° (vertical upward pipe) and depicted in Figure 9. These probabilistic maps represent encouraging tools for rejecting possible flow

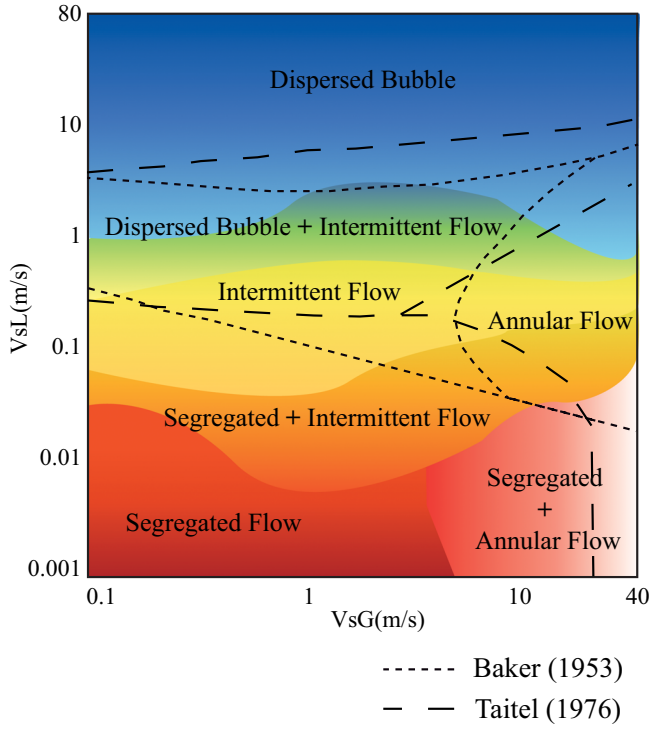

Fig. 10. Comparison between flow pattern maps for horizontal pipelines with the maps of Baker [2] and Taitel and Dukler [10].

patterns under a high level of probability in an experimental dataset. Note that stratified and annular flow patterns do not have significant contributions for the same inclination, which suggest a significant result in the calculation of the error rate for further experimental assessments. Besides, there is an interesting behavior in the intermittent flow pattern, which is favored by upward vertical pipes in comparison to horizontal pipes; however, for the downward case (−90°), this is not the case, and an annular flow is favored due to the gas properties. Figure 9 also shows that the probabilities of belonging to annular (for 0°) and intermittent (for −90°) flow patterns seem to be negligible; nevertheless, these probabilities are 0.25 and 0.05, respectively.

Finally, the obtained flow pattern map is compared with two commonly used flow maps used in industry (Baker [2] and Taitel and Dukler [10]) in Figure 10. The map proposed in this work uses transition zones not as boundaries, but as a probability area where there may be more than one pattern at the same time. Besides, maps found in the literature are generally applicable to experimental conditions under specific operating and pipe configurations. On the contrary, the approach proposed in this work was generated from a significant experimental and synthetic dataset, so a broader number of cases may be applicable.

5 Conclusion and future perspectives

A probabilistic flow pattern map is proposed for liquid-gas phase flow pipelines based on a comprehensive experimental dataset and synthetic records obtained from OLGA. This map aims to predict probable flow regimes given gas and liquid superficial velocities and to evaluate possible transition zones among them, which are sought to replace traditional transition boundaries. This map was developed for several inclinations upward and downward from −90° to 90° with steps of 5°.

To build this flow pattern map, acceptable records from the experimental dataset were selected using a tolerable error from synthetic records and their reported void fraction. For those records lacking this parameter, a supervised learning process was proposed to complete this classification. For this purpose, two learning techniques (*i.e.*, SVM and KKN) were considered. Finally, a Bayesian approach was considered based on the available information and the overlapping information from the experimental and synthetic datasets.

The proposed approach is an alternative to the current flow pattern maps, which are somehow limited to the configurations under they are developed. The synthetic records were determined using random properties from OLGA subjected to the ranges obtained from the experimental dataset. Similar approaches can be proposed using different simulation software, bearing in mind the uncertainty surrounding the experiments and simulations. In case new records are added to the current database, a robust tool can be proposed. For instance, data can be extrapolated to cover a wider number of tilt angles and not only every 5°.

Acknowledgments. The authors gratefully acknowledge *Schlumberger* for providing the OLGA as well acknowledge Prof. Eduardo Pereyra (University of Tulsa) for the help, advice, and guidance with the study. Finally, the authors want to acknowledge Prof. Rodrigo Marin (Universidad de los Andes) for his continued assistance with the Schlumberger software.

Supplementary Material

Supplementary Material is available at https://ogst.ifpenergiesnouvelles.fr/10.2516/ogst/2019034/olm

References

1 Dalkilic A.S., Wongwises S. (2010) An investigation of a model of the flow pattern transition mechanism in relation to the identification of annular flow of R134a in a vertical tube using various void fraction models and flow regime maps, *Exper. Therm. Fluid Sci.* **34**, 6, 692–705. doi: 10.1016/j.expthermflusci.2009.12.011.

2 Baker O. (1953) Design for simultaneous flow of oil and gas, in: *Fall meeting of the petroleum branch of AIME*, Society of Petroleum Engineers, Dallas, USA, 856–863. doi: 10.2118/323-G.

3 Cheng L., Ribatski G., Wojtan L., Thome J.R. (2006) New flow boiling heat transfer model and flow pattern map for carbon dioxide evaporating inside horizontal tubes, *Int. J. Heat Mass Trans.* **49**, 21, 4082–4094. doi: 10.1016/j.ijheatmasstransfer.2006.04.003.

4 Kattan N., Thome J.R., Favrat D. (1998) Flow boiling in horizontal tubes. Part 1: Development of a diabatic

two-phase flow pattern map, *J. Heat Trans.* **120**, 1, 140–147. doi: 10.1115/1.2830037.
5 Kattan N., Thome J.R., Favrat D. (1998) Flow boiling in horizontal tubes: Part 2 – New heat transfer data for five refrigerants, *J. Heat Trans.* **120**, 1, 148–155. doi: 10.1115/1.2830038.
6 Kattan N., Thome J.R., Favrat D. (1998) Flow boiling in horizontal tubes: Part 3 – Development of a new heat transfer model based on flow pattern, *J. Heat Trans.* **120**, 1, 155–165. doi: 10.1115/1.2830039.
7 Ghajar A.J., Tang C.C. (2007) Heat transfer measurements, flow pattern maps, and flow visualization for non-boiling two-phase flow in horizontal and slightly inclined pipe, *Heat Trans. Eng.* **28**, 6, 525–540. doi: 10.1080/01457630701193906.
8 Ghajar A.J. (2005) Non-boiling heat transfer in gas-liquid flow in pipes: A tutorial, *J. Braz. Soc. Mech. Sci. Eng.* **27**, 46–73. doi: 10.1590/S1678-58782005000100004.
9 Shoham O. (1982) Flow pattern transition and characterization in gas-liquid two phase flow in inclined pipes, *PhD Thesis*, Tel-Aviv University.
10 Taitel Y., Dukler A.E. (1976) A model for predicting flow regime transitions in horizontal and near horizontal gas-liquid flow, *AIChE J.* **22**, 1, 47–55. doi: 10.1002/aic.690220105.
11 Hewitt G.F., Roberts D.N. (1969) *Studies of two-phase flow patterns by simultaneous X-ray and flash photography*, Technical report, Atomic Energy Research Establishment, Harwell, UK.
12 Cheng L., Ribatski G., Thome J.R. (2008) Two-phase flow patterns and flow-pattern maps: Fundamentals and applications, *Appl. Mech. Rev.* **61**, 5, 1–28. doi: 10.1115/1.2955990.
13 Govier G.W., Radford B.A., Dun J.S.C. (1957) The upwards vertical flow of air–water mixtures – effect of air and water rates on flow pattern, holdup and pressure gradient, *Can. J. Chem. Eng.* **35**, 58–70.
14 Griffith P., Wallis G.B. (1961) Two-phase slug flow, *Trans. ASME. J. Heat Transfer* **83**, 307–320.
15 Golan L.P., Stenning A.H. (1969–1970) Two-phase vertical flow maps, *Proc. Inst. Chem. Engrs.* **184**, Pt-3.
16 Oshinowo T., Charles M.E. (1974) Vertical two-phase flow. Flow pattern correlations, *Can. J. Chem. Eng.* **52**, 25–35.
17 Taitel Y., Barnea D., Dukler A.E. (1980) Modelling flow pattern transitions for steady upward gas–liquid flow in vertical tubes, *AIChE J.* **26**, 345–354.
18 Spedding P.L., Nguyen V.T. (1980) Regime maps for air–water two-phase flow, *Chem. Eng. Sci.* **35**, 779–793.
19 Barnea D., Shoham O., Taitel Y. (1982) Flow pattern transition for vertical downward two phase flow, *Chem. Eng. Sci.* **37**, 741–744.
20 Spisak W. (1986) Two-phase flow of gas-highly viscous liquid, *PhD Thesis*, Wroclaw Technical University, Poland.
21 Ulbrich R. (1989) Two-phase gas–liquid flow identification, *Studies and Monographs* **32**, WSI Opole.
22 Dziubinski M., Fidos H., Sosno M. (2004) The flow pattern map of a two-phase non-Newtonian liquid-gas flow in the vertical pipe, *Int. J. Multiph. Flow* **30**, 6, 551–563. doi: 10.1016/j. ijmultiphaseflow.2004.04.005.
23 Baker O. (1954) Design of Pipe Lines for Simultaneous Flow of Oil and Gas, *Oil Gas J.* **26**, July.
24 Hashizume K. (1983) Flow Pattern and Void Fraction of Refrigerant Two-Phase Flow in a Horizontal Pipe, *Bull. JSME* **26**, 219, 1597–1602.
25 Steiner D. (1993) in *Heat Transfer to Boiling Saturated Liquids, VDI-Warmeatlas (VDI Heat Atlas)*, Verein Deutscher Ingenieure (VDI), Gessellschaft Verfahrenstechnik und Chemieingenieurwesen (GCV), (ed) Fullarton J.W., trans., Dusseldorf.
26 Thome J.R., El Hajal J. (2003) Two-phase flow pattern map for evaporation in horizontal tubes: Latest version, *Heat Trans. Eng.* **24**, 6, 3–10. doi: 10.1080/714044410.
27 Magrini K.L. (2009) Liquid entrainment in annular gas-liquid flow in inclined pipes, *Master's Thesis*, The University of Tulsa, Tulsa, USA.
28 Mukherjee H. (1979) An experimental study of inclined two-phase flow, *PhD Thesis*, The University of Tulsa, Tulsa, USA.
29 Wu B., Firouzi M., Mitchell T., Rufford T.E., Leonardi C., Towler B. (2017) A critical review of flow maps for gas-liquid flows in vertical pipes and annuli, *Chem. Eng. J.* **326**, 350–377. doi: 10.1016/jxej.2017.05.135. http://www.sciencedirect.com/science/article/pii/S1385894717308938.
30 Bendiksen K.H. (1991) The dynamic two-fluid model OLGA: Theory and application, *Soc. Pet. Eng.* **6**, 2, 171–180. doi: 10.2118/19451-PA.SPE-19451-PA.
31 Larsen M., Hustvedt E., Hedne P., Straume T. (1997) PeTra: A novel computer code for simulation of slug flow, in: *SPE Annual Technical Conference and Exhibition*, 5–8 October, San Antonio, Texas. doi: 10.2118/38841-MS.
32 Belt R., Duret E., Larrey D., Djoric B., Kalali S. (2011) Comparison of commercial multiphase flow simulators with experimental and field databases, in: *15th International Conference on Multiphase Production Technology*, Society of Petroleum Engineers, Cannes, France.
33 Smith I.E., Krampa F.N., Fossen M., Brekken C., Unander T.E. (2011) Investigation of horizontal two-phase gas-liquid pipe flow using high viscosity oil: Comparison with experiments using low viscosity oil and simulations, in: *15th International Conference on Multiphase Production Technology*, Society of Petroleum Engineers, Cannes, France.
34 Johnson G.W., Kjeldby T.B., Nydal O.J. (2011) A Comparison of slug and wave characteristics in high pressure flow with multiphase models, in: *15th International Conference on Multiphase Production Technology*, Society of Petroleum Engineers, Cannes, France.
35 Archibong-Eso A., Yan W., Baba Y., Kanisho S., Yeung H. (2015) Viscous liquid-gas flow in horizontal pipelines: Experiments and multiphase flow simulator assessment, in: *17th International Conference on Multiphase Production Technology*, Society of Petroleum Engineers, Cannes, France.
36 Choi J., Pereyra E., Sarica C., Lee H., Jang I.L., Kang J. (2013) Development of a fast transient simulator for gas-liquid two- phase flow in pipes, *J. Pet. Sci. Eng.* **102**, 27–35. doi: 10.1016/j.petrol.2013.01.006.
37 Ali S.F. (2009) Two phase flow in large diameter vertical riser, *PhD Thesis*, School of Engineering, Cranfield University.
38 Canière H., T'Joen C., De Paepe M. (2008) Towards objective flow pattern mapping with the k-means clustering algorithm, in: *Proceedings of the Sixth International Conference on Heat Transfer, Fluid Mechanics & Thermodynamics – HEFAT 2008*, 30 June – 2 July 2008, Pretoria, South Africa.
39 Niño V.G. (2002) Characterization of two-phase flow in microchannels, *PhD Thesis*, Urbana and Champaign, Champaign, USA.

40 Jassim E.W., Newell T.A. (2006) Prediction of two-phase pressure drop and void fraction in microchannels using probabilistic flow regime mapping, *Int. J. Heat Mass Trans.* **49**, 15, 2446–2457. doi: 10.1016/j.ijheatmasstransfer.2006.01.034.

41 Jassim E.W., Newell T.A., Chato J.C. (2007) Probabilistic determination of two-phase flow regimes in horizontal tubes utilizing an automated image recognition technique, *Exper. Fluids* **42**, 4, 563–573. doi: 10.1007/s00348-007-0264-8.

42 Canière H., Bauwens B., T'Joen C., De Paepe M. (2009) Probabilistic mapping of adiabatic horizontal two-phase flow by capacitance signal feature clustering, *Int. J. Multiph. Flow* **35**, 7, 650–660. doi: 10.1016/j.ijmultiphaseflow.2009.03.006.

43 Canière H., Bauwens B., T'Joen C., De Paepe M. (2010) Mapping of horizontal refrigerant two-phase flow patterns based on clustering of capacitive sensor signals, *Int. J. Heat Mass Trans.* **53**, 23, 5298–5307. doi: 10.1016/j.ijheatmasstransfer.2010.07.027.

44 França F., Lahey R.T. (1992) The use of drift-flux techniques for the analysis of horizontal two-phase flows, *Int. J. Multiph. Flow* **18**, 6, 787–801. doi: 10.1016/0301-9322(92)90059-P.

45 Zhang H.-Q., Wang Q., Sarica C., Brill J.P. (2003) Unified model for gas-liquid pipe flow via slug dynamics – Part 1: Model development, *J. Energy Res. Technol.* **125**, 4, 266–273. doi: 10.1115/1.1615246.

46 Fan Y. (2005) An Investigation of low liquid loading gas-liquid stratified flow in near-horizontal pipes, *PhD Thesis*, The University of Tulsa, Tulsa, USA.

47 Meng W. (2000) Low liquid loading gas-liquid two-phase flow in near horizontal pipes, *PhD Thesis*, The University of Tulsa, Tulsa, USA.

48 Thome J.R. (2004) *Void fractions in two-phase flows, chapter 17*, Wolverine Tube Inc, Alabama, USA, 1–33. doi: 10.1002/ 0471465186.ch11.

49 Inoue E.H., Carvalho R., Estevam V., Bannwart A.C., Frattini M., Fileti A. (2013) Development of a neural network for the identification of multiphase flow patterns, in: *Proceedings of the IASTED International Conference*, Marina del Rey, USA.

50 Carey V.P. (1993) Two-phase flow in small-scale ribbed and finned passages for compact evaporators and condensers, *Nucl. Eng. Des.* **141**, 1, 249–268. doi: 10.1016/0029-5493(93)90105-I.

51 Falcone G., Hewitt G.F., Alimonti C. (2009) *Multiphase Flow metering, volume 54 of developments in petroleum science*, Elsevier, Amsterdam, The Netherlands. doi: 10.1016/S0376-7361(09)05413-2.

52 Kouba G. (1986) Horizontal slug flow modelling and metering, *PhD Thesis*. The University of Tulsa, Tulsa, USA.

53 Thomas J.E. (2004) *Fundamentos de engenharia de petróleo*, Interciência, Rio de Janeiro, Brazil, ISBN 9788571930995.

54 Omebere-Iyari N.K., Azzopardi B.J. (2007) A study of flow patterns for gas/liquid flow in small diameter tubes, *Chem. Eng. Res. Des.* **85**, 2, 180–192. doi: 10.1205/cherd05059.

55 Rosa E.S., Salgado R.M., Ohishi T., Mastelari N. (2010) Performance comparison of artificial neural networks and expert systems applied to flow pattern identification in vertical ascendant gas-liquid flows, *Int. J. Multiph. Flow* **36**, 9, 738–754. doi: 10.1016/j.ijmultiphaseflow.2010.05.001.

56 Abduvayt P., Arihara N., Manabe R., Ikeda K. (2003) Experimental and modeling studies for gas-liquid two-phase flow at high pressure conditions, *J. Jpn. Pet. Inst.* **46**, 2, 111–125. doi: 10.1627/jpi.46.111.

57 Badie S., Hale C.P., Lawrence C.J., Hewitt G.F. (2000) Pressure gradient and holdup in horizontal two-phase gas-liquid flows with low liquid loading, *Int. J. Multiph. Flow* **26**, 9, 1525–1543. doi: 10.1016/S0301-9322(99)00102-0. http://www.sciencedirect.com/science/article/pii/S0301932299001020.

58 Beggs H.D. (1972) An experimental study of two-phase flow in inclined pipes, *PhD Thesis*, The University of Tulsa, Tulsa, USA.

59 Carvalho R.D.M., Venturini O.J., Tanahashi E.I., Neves F., Franga F.A. (2009) Application of the ultrasonic technique and high-speed filming for the study of the structure of air-water bubbly flows, *Exper. Therm. Fluid Sci.* **33**, 7, 1065–1086. doi: 10.1016/j.expthermflusci.2009.06.004.

60 Felizola H. (1992) Slug flow in extended research directional wells, *Master's Thesis*, The University of Tulsa, Tulsa, USA.

61 Gokcal B. (2008) An experimental and theoretical investigation of slug flow for high oil viscosity in horizontal pipes, *PhD Thesis*, The University of Tulsa, Tulsa, USA.

62 Majumder S.K., Ghosh S., Mitra A.K., Kundu G. (2010) Gas- Newtonian and gas-non-Newtonian slug flow in vertical pipe, Part I: Gas holdup characteristics, *Int. J. Chem. React. Eng.* **8**, 1, 1–23, Article A117.

63 Manabe R., Zhang H.-Q., Delle-Case E., Brill J. (2001) Crude oil-natural gas two-phase flow pattern transition boundaries at high pressure conditions, in: *SPE Annual Technical Conference and Exhibition*, Society of Petroleum Engineers, New Orleans, Louisiana.

64 Roumazeilles R. (1994) An experimental study of downward slug flow in inclined pipes, *Master's Thesis*, The University of Tulsa, Tulsa, USA.

65 Schmidt J., Giesbrecht H., van der Geld C.W.M. (2008) Phase and velocity distributions in vertically upward high--viscosity two-phase flow, *Int. J. Multiph. Flow* **34**, 4, 363–374. doi: 10.1016/j.ijmultiphaseflow.2007.10.013.

66 Tanahashi E.I., Abud-Jr J.R., Carvalho R.D., Venturini F., Neves-Jr O.J., Franga F.A. (2009) Development of an ultrasonic apparatus for the study of the structure of air-water bubbly flows and the determination of the void fraction, in: *Proceedings of the 7th World Conference on Experimental Heat Transfer, Fluid Mechanics and Thermodynamics*, June 28–July 03, Krakow.

67 Wilkens R.J. (1997) Prediction of the flow regime transitions in high pressure, large diameter, inclined multiphase pipelines, *PhD Thesis*, Ohio University.

68 Kawahara A., Chung P.M.-Y., Kawaji M. (2002) Investigation of two-phase flow pattern, void fraction and pressure drop in a microchannel, *Int. J. Multiph. Flow* **28**, 9, 1411–1435. doi: 10.1016/S0301-9322(02)00037-X.

69 Triplett K.A., Ghiaasiaan S.M., Abdel-Khalik S.I., LeMouel A., McCord B.N. (1999) Gas-liquid two- phase flow in microchannels: Part II: Void fraction and pressure drop, *Int. J. Multiph. Flow* **25**, 3, 395–410. doi: 10.1016/S0301-9322(98)00055-X. http://www.sciencedirect.com/science/article/pii/S030193229800055X.

70 Tarca L.A., Grandjean B.P.A., Larachi F. (2004) Designing supervised classifiers for multiphase flow data classification, *Chem. Eng. Sci.* **59**, 16, 3303–3313. doi: 10.1016Zj.ces.2004.05.005.

71 Zhang L., Wang H. (2010) Identification of oil-gas two-phase flow pattern based on SVM and electrical capacitance tomography technique, *Flow Meas. Instrum.* **21**, 1, 20–24. doi: 10.1016/j.flowmeasinst.2009.08.006.

72 Youn E., Koenig L., Jeong M.K., Baek S.H. (2010) Support vector-based feature selection using Fisher's linear discriminant and support vector machine, *Expert Syst. Appl.* **37**, 9, 6148–6156. doi: 10.1016/j.eswa.2010.02.113.

73 Sigut M., Alayón S., Hernández E. (2014) Applying pattern classification techniques to the early detection of fuel leaks in petrol stations, *J. Clean. Prod.* **80**, 262–270. doi: 10.1016/j.jclepro.2014.05.070.

74 Duda R.O., Hart P.E., Stork D.G. (2012) *Pattern classification*, Wiley, New York, USA. ISBN 9781118586006.

75 Hsu C.-W., Chang C.-C., Lin C.-J. (2003) *A practical guide to support vector classification*, National Taiwan University, Taipei, Taiwan.

76 Schlumberger (2013) *OLGA dynamic multiphase Flow simulator. User Manual, Version 7.3.3.* Technical Report, Schlumberger Limited.

77 Pereyra E., Torres C., Mohan R., Gomez L., Kouba G., Shoham O. (2012) A methodology and database to quantify the confidence level of methods for gas-liquid two-phase flow pattern prediction, *Chem. Eng. Res. Des.* **90**, 4, 507–513. doi: 10.1016/j.cherd.2011.08.009.